Supplementary Information (SI) for RSC Advances.
This journal is © The Royal Society of Chemistry 2025

Supporting Information

In Situ Transformation of Pd to Metal-metalloid Alloy Pd_2B for Alkyne Semi-hydrogenation

Shuaiwen Xu[a], Lei Wang[a], Pengfei Tian[b], and Shenghu Zhou*[a]

[a] Shanghai Key Laboratory of Multiphase Materials Chemical Engineering, School of Chemical Engineering. East China University of Science and Technology, 130 Meilong Road, Shanghai 200237, P. R. China.

[b] Key Laboratory of Pressure Systems and Safety, Ministry of Education, School of Mechanical and Power Engineering. East China University of Science and Technology, 130 Meilong Road, Shanghai 200237, P. R. China.

***Corresponding authors:**

Fax: (+86) 21-64253159 for S. Zhou.

E-mail: zhoushenghu@ecust.edu.cn.

Chemicals. Palladium chloride ($PdCl_2$), ethylene glycol (EG, ≥ 99 %) and tetrahydrofuran (THF, ≥ 99.0 %) were purchased from Aladdin. Polyvinyl pyrrolidone (PVP-K30) was purchased from Shanghai Chemical Reagent Co.. Borane dimethylamine complex (DMAB, 96 %) was purchased from Shanghai Zhonghe Chemical Technology Co., Ltd.. Aluminum oxide powders were purchased from Qingdao Haiyang Chemical Co., Ltd.. Methanol anhydrous (MeOH, ≥ 99.5 %), ethanol absolute (EtOH, ≥ 99.7 %) and acetone (ACE, ≥ 99.5 %) were purchased from Sinopharm Chemical Reagent Co., Ltd.. Propan-2-ol (IPA, ≥ 99.5 %), 1-butanol (BA, ≥ 99.5 %) were purchased from Shanghai Boer Chemical Reagents Co., Ltd.. 3-hexyne-1-ol (HY, 97 %), *cis*-3-hexen-1-ol (*cis*-HE, ≥ 99%), (*E*)-hex-3-en-1-ol (*trans*-HE, 97%), 1-hexanol (HA, 98 %), 2-butyn-1-ol (BY, ≥ 97 %), crotyl alcohol (BE, ≥ 95 %), diphenylacetylene (DPA, 99 %), *cis*-stilbene (*Z*-ST, 97 %), (*E*)-1,2-diphenylethene (*E*-ST, 98 %) and 1,2-diphenylethane (DPE, ≥ 98 %) were purchased from Shanghai Titan Technology Co., Ltd.. All of the reagents were used as received without further purification.

Materials Characterization. The images of transmission electron microscopy (TEM) were obtained on a JEM-2100 transmission electron microscope operated at an acceleration voltage of 200 kV. X-ray powder diffraction (XRD) patterns were recorded on a Bruker D8 Advance diffractometer using Cu-Kα radiation in the 2θ degree range from 10° to 80°. The actual metal loadings of various materials were determined by an Agilent 725 inductively coupled plasma optical emission spectrometer (ICP-OES). The

analysis of X-ray Photon-electron Spectroscopy (XPS) for various samples were obtained using a Thermo Scientific ESCALAB 250Xi. High angle annular dark field-scanning transmission electron microscopy (HAADF-STEM) images with energy dispersive spectroscopy (EDS) phase mapping and line-scans were obtained using a Talos F200x, operated at 200 kV for STEM Model. The diffuse reflectance Fourier transform infrared spectra (DRIFT-IR) with CO probes were obtained using a Nicolet NEXUS-470 Fourier transform infrared spectrometer.

The GC analysis of reaction solution by external standard method. Relative response factors of components and their surface areas in GC chromatograms are used to calculate conversions and selectivity. After hydrogenation, relative surface areas of components in product samples are first obtained, and then known amount of reactants are added into the samples if the conversions is high or known amount of products are added into the samples if the conversions is low. Reactant conversions and main product selectivity are calculated from the relative response factors of components, and GC chromatograms of samples and samples with a known amount of reactants or main products.

Computational models and methods. DFT calculations were performed using the Vienna ab-initio simulation package (VASP).[1,2] A plane-wave basis set with a cut-off energy of 450 eV was used to expand the Kohn-Sham wave functions. The interactions between the ionic cores and valence electrons were described using a

projector augmented wave (PAW) method,[3,4] and the exchange-correlation effects were self-consistently described within the Perdew-Burke-Ernzerh of generalized gradient approximation (GGA-PBE).[5,6] The occupation of electronic states was determined using Gaussian smearing method[7] and the smearing width was 0.01 eV. DFT-D3 approach was used to describe van der Waals interaction.[8]

Pd (111) and Pd_2B (001) surfaces were modeled as four-layered slab with (5×5) and (4×4) unit cells, respectively. The bottom layer of Pd (111) and Pd_2B (001) was fixed, and the rest layers as well as the surface species were fully relaxed. A vacuum spacing of 12 Å along the normal direction (z) to the surface and 1×1×1 Gamma centered k-point sampling were used for all the models. Optimized geometries were obtained by minimizing the maximum force on any ion until it is less than 0.05 eV/Å.

To calculate the energy barrier for the elementary reactions, the transition states were found using the climbing image nudged elastic band (NEB) method[9] and the dimer method,[10] confirmed via vibrational analysis.

The binding energies (BEs) of surface species were calculated as:

$$BE = E_{adsorbate/surface} - E_{clean} - E_{adsorbate} \qquad (1)$$

where $E_{adsorbate/surface}$, E_{clean}, and $E_{adsorbate}$ are the total energies of the catalyst substrate with the adsorbate, the clean catalyst substrate without the adsorbed species, and the neutral adsorbate species in the gas phase, respectively.

The reaction energy (ΔE) for the elementary steps was calculated using the following equation:

$$\Delta E = E_{FS} - E_{IS} \qquad (2)$$

where E_{FS} and E_{IS} are the total energies of the final state (FS) and initial state (IS) of the minimum-energy path (MEP), respectively. The activation energy barrier (E_a) was calculated equation (3):

$$E_a = E_{TS} - E_{IS} \quad (3)$$

where E_{TS} is the energy of the transition state (TS) of MEP.

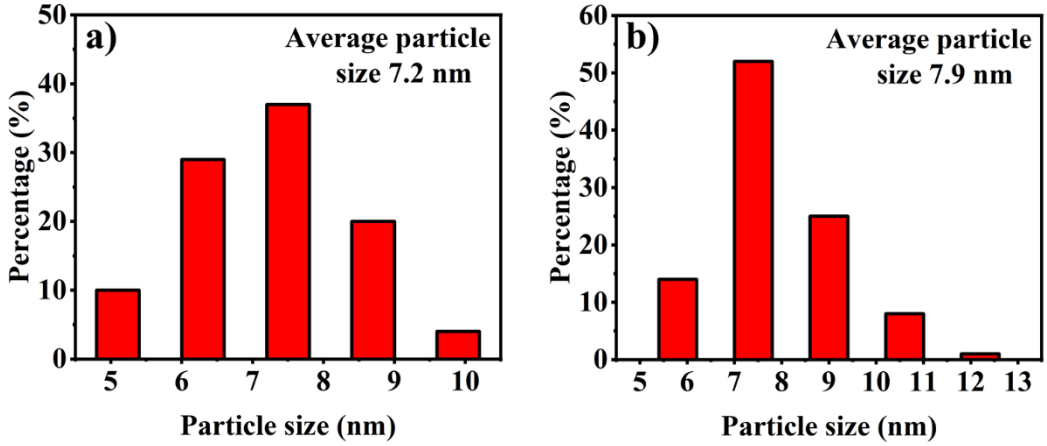

Fig. S1. Size distributions of a), Pd/Al_2O_3 and b), Pd_2B/Al_2O_3.

Table S1. The metal loadings of various materials determined by ICP-OES and the atomic molar ratios of species with different valance states by XPS analysis.

Samples	Pd loading (wt%)	B loading (wt%)	Molar ratios	
			Pd^0/Pd^{2+}	$B^0/B\text{-}O_x$
Pd/Al_2O_3	2.9	N/A	74.2/25.8	N/A
Pd_2B/Al_2O_3	2.6	2.5	81.4/18.6	21.2/78.8

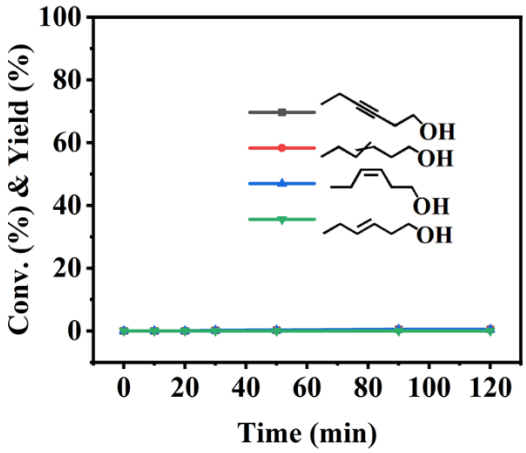

Fig. S2. Reaction profiles of HY hydrogenation over B_xO_y/Al_2O_3. Reaction conditions: HY, 1.0 mmol; MeOH 10.0 mL; reaction temperature, 30 °C; speed of agitation, 700 rpm; H_2 pressure, 0.1 MPa; B_xO_y/Al_2O_3, 4.1 mg. The synthetic procedures of B_xO_y/Al_2O_3 were same as those of Pd_2B/Al_2O_3 except that individual alumina (not Pd/Al_2O_3) were used. The B loading of B_xO_y/Al_2O_3 determined by ICP-OES is 2.1 wt%.

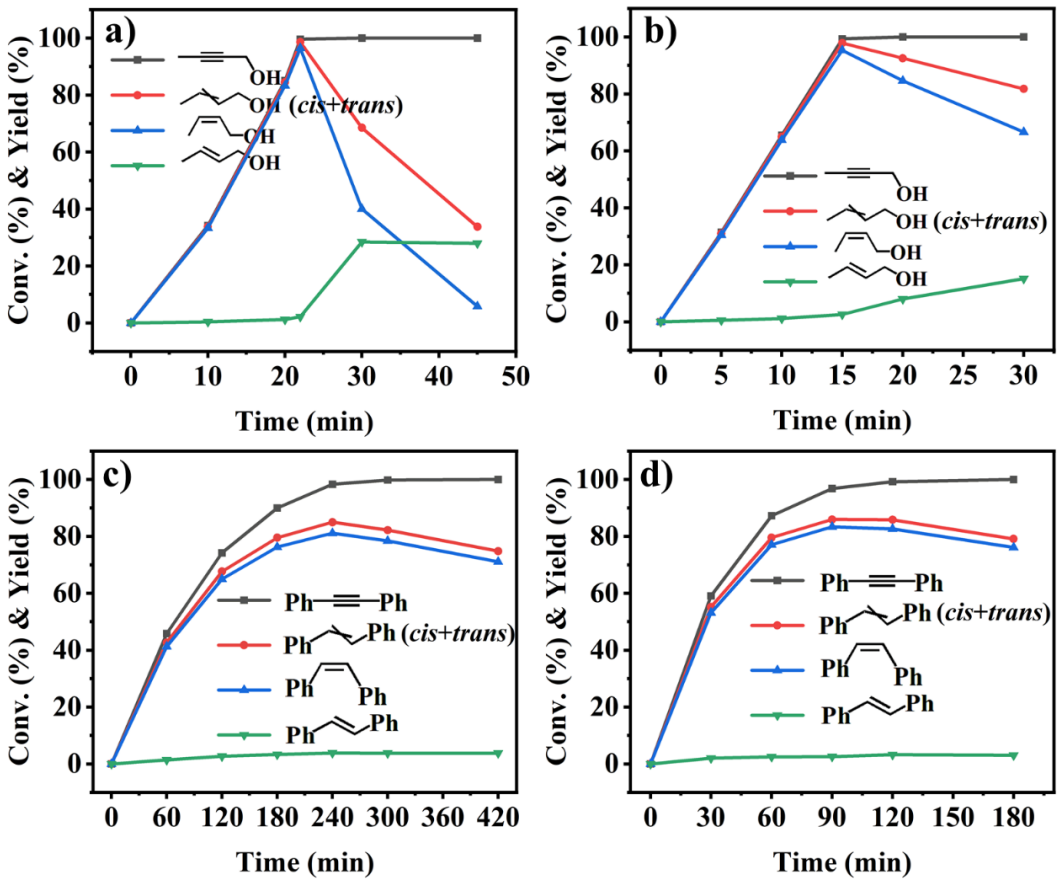

Fig. S3. Reaction profiles of BY hydrogenation over: a), Pd/Al_2O_3; b), Pd_2B/Al_2O_3. Reaction profiles of DPA hydrogenation over: c), Pd/Al_2O_3; d), Pd_2B/Al_2O_3. Reaction conditions: substrate/Pd molar ratio, 500/1; substrate, 0.5 mmol; EtOH, 10.0 mL; reaction temperature, 45 °C; speed of agitation, 700 rpm; H_2 pressure, 0.1 MPa. Red curves are the yields of alkene including *cis*- and *trans*-alkene.

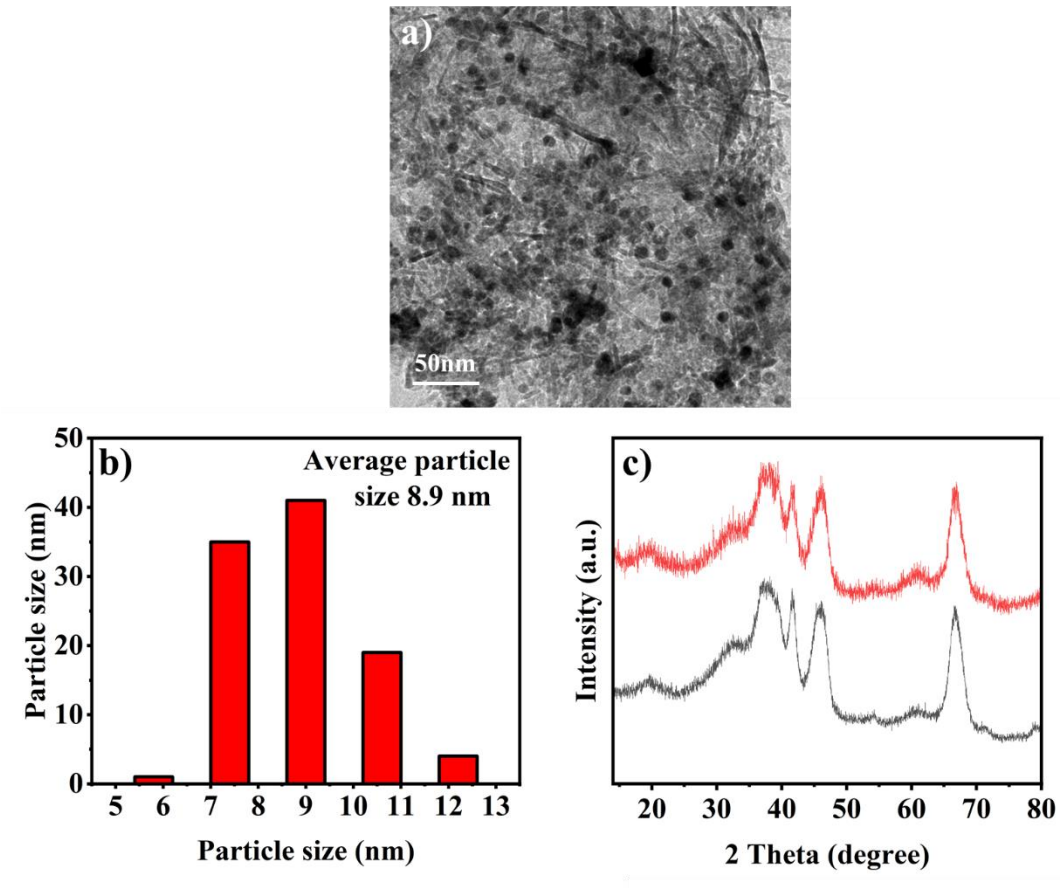

Fig. S4. The recycled Pd_2B/Al_2O_3: a), TEM images; b), particle size distribution of NPs; c), XRD pattern of fresh (black) and recycled Pd_2B/Al_2O_3 (red).

Table S2. The comparison of catalytic performance between this work and the reported ones for 3-hexyne-1-ol semi-hydrogenation.

Catalysts	Alkynes Conv. (%)	Alkenes Sel. (%) *cis*/*trans*	Selectivity maintenance	Reaction conditions	Ref.
5% Pd/C (Johnson Matthey)	100.0	0	No	3 bar, 30 °C	11
PdGluC400[O]H_2O_2/NH_4OH	100.0	91.9 91.5/8.5	Yes	3 bar, 30 °C	11
3% Pd-^{int}B/C	97.0	99.8 98/2	Yes	3 bar, 30 °C	12
Lindlar	>99.0	99.0 97/3	No	3 bar, 30 °C	13
c-Pd/TiS	97.0	99.0 97/3	Yes	3 bar, 30 °C	13
[PdCu]	96.0	99.0 98/2	No	3 bar, 25 °C	14
AgPd@SiO_2	43.0	90.7	No	ambient H_2, [a]RT	15
Pd-PVP 1 w/w%	98.0	>96.0 >96/4	No	0.1 MPa, 25 °C	16
Pd@Ag-0.20	>99.0	>99.0 100/0	No	1 atm, [a]RT	17
Pd@MPSO/SiO_2-1	>99.0	99.0 98/2	Yes	1 atm, 30°C	18
Pd_2B/Al_2O_3	99.8	96.2 97/3	Yes	0.1 MPa, 30 °C	This work

[a]Room tempertature.

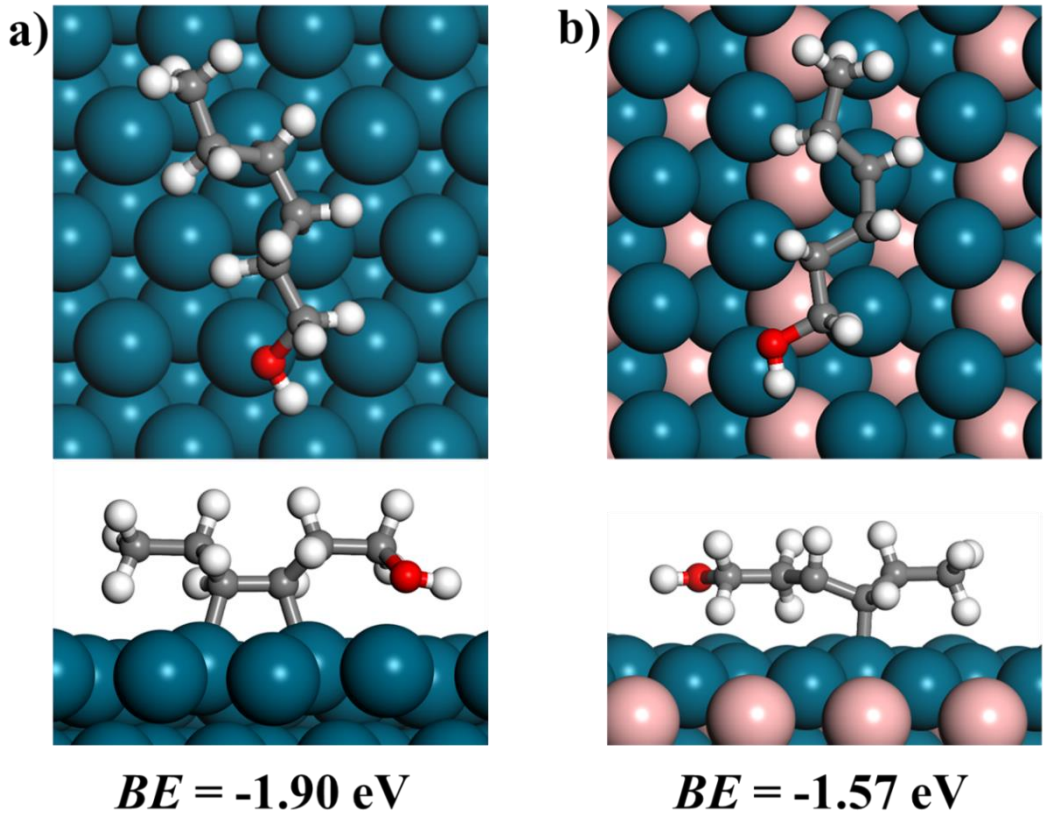

Fig. S5. The top and side view of the adsorption configurations of HE on a) Pd (111) and b) Pd_2B (001). Pd, blue; B, pink; C, gray; O, red; H, white.

References

1. G. Kresse and J. Furthmüller, *Phys Rev B Condens Matter*, 1996, **54**, 11169-11186.
2. G. Kresse and J. Furthmüller, *Comput. Mater. Sci.,* 1996, **6**, 15-50.
3. P. E. Blöchl, *Phys Rev B Condens Matter,* 1994, **50**, 17953-17979.
4. G. Kresse and D. Joubert, *Phys Rev B*, 1999, **59**, 1758-1775.
5. J. P. Perdew and W. Yue, *Phys Rev B Condens Matter*, 1986, **33**, 8800-8802.
6. J. P. Perdew, K. Burke, and M. Ernzerhof, *Phys. Rev. Lett.* 1996, **77**, 3865-3868.
7. M. Methfessel and A. T. Paxton, *Phys Rev B Condens Matter*, 1989, **40**, 3616-3621.
8. S. Grimme, J. Antony, S. Ehrlich and H. Krieg, *J. Chem. Phys.*, 2010, **132**, 154104.
9. G. Henkelman, B. P. Uberuaga and H. Jónsson, *J. Chem. Phys.,* 2000, **113**, 9901-9904.
10. G. Henkelman, and H. Jónsson, *J. Chem. Phys.* 1999, **111**, 7010-7022.
11. C. W. Chan, Y. Xie, N. Cailuo, K. M. Yu, J. Cookson, P. Bishop and S. C. Tsang, *Chem. Commun.*, 2011, **47**, 7971-7973.
12. C. W. Chan, A. H. Mahadi, M. M. Li, E. C. Corbos, C. Tang, G. Jones, W. C. Kuo, J. Cookson, C. M. Brown, P. T. Bishop and S. C. Tsang, *Nat. Commun.*, 2014, **5**, 5787.
13. P. T. Witte, P. H. Berben, S. Boland, E. H. Boymans, D. Vogt, J. W. Geus and J. G. Donkervoort, *Top. Catal.*, 2012, **55**, 505-511.

14. W. Oberhauser, M. Frediani, I. Mohammadi Dehcheshmeh, C. Evangelisti, L. Poggini, L. Capozzoli and P. Najafi Moghadam, *ChemCatChem*, 2022, DOI：10.1002/cctc.202101910

15. V. Sudheeshkumar, M. Alyari, M. Gangishetty and R. W. J. Scott, *Catal. Sci. Technol.*, 2020, **10**, 8421-8428.

16. C. Evangelisti, N. Panziera, A. D'Alessio, L. Bertinetti, M. Botavina and G. Vitulli, *J. Catal.*, 2010, **272**, 246-252.

17. T. Mitsudome, T. Urayama, K. Yamazaki, Y. Maehara, J. Yamasaki, K. Gohara, Z. Maeno, T. Mizugaki, K. Jitsukawa and K. Kaneda, *ACS Catal.*, 2015, **6**, 666-670.

18. T. Mitsudome, Y. Takahashi, S. Ichikawa, T. Mizugaki, K. Jitsukawa and K. Kaneda, *Angew. Chem. Int. Ed. Engl.*, 2013, **52**, 1481-1485.